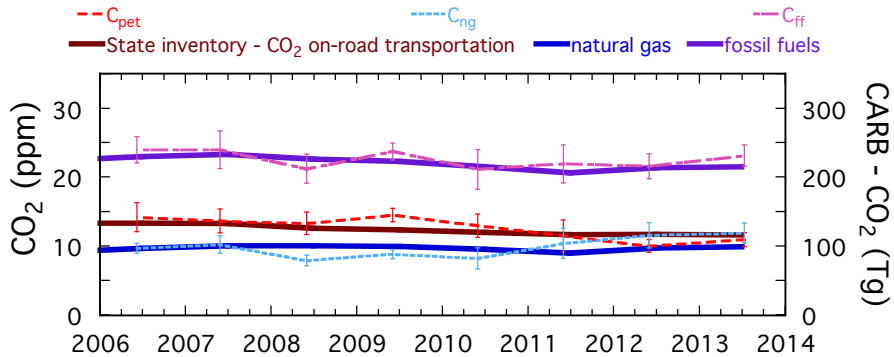


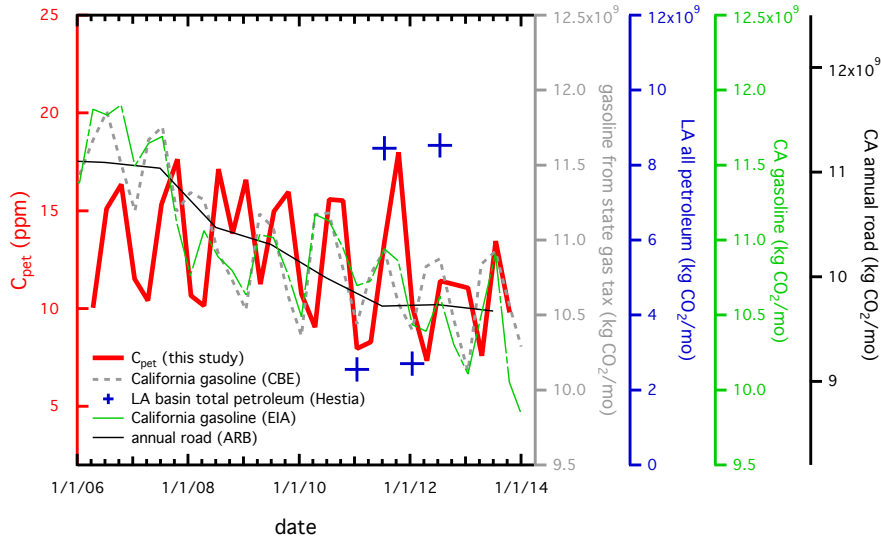
1057 | Figure 10. Results of ensemble empirical mode decomposition (EEMD) (Huang et al.,
1058 | 1998; Wu and Huang, 2009) of the C_{ff} time series calculated using Eq. (3) and the
1059 | average, constant $\Delta^{14}\text{C}$ of -954 ‰ for fossil fuel. The top set of panels show the raw data
1060 | (a), noise (b), annual and semi-annual mode (c), and the trend + IMF 6 (d). The pattern
1061 | of the trend + IMF 6 shown in (d) is within 1σ uncertainty of no variation over this time
1062 | period. The bottom two panels include the raw data after subtracting the average annual
1063 | cycle (centered at zero) (e) and the trend + IMF 6 for the modified data set (f). 30-day
1064 | average temperatures (minus the overall average and scaled to match the magnitude of
1065 | the C_{ff} IMF; blue curve) are superimposed on the plot of IMF 3 + IMF 4 (c). Shaded
1066 | regions in (f) indicate 1σ standard deviation of 300 Monte Carlo realizations with 13.7 %
1067 | noise added, the ratio of the uncertainty in C_{ff} to the standard deviation of the data.

Unknown

Formatted: Font:Times, Bold



1068 Figure 11. Comparison of annual average CO₂ emissions from bottom-up California Air
 1069 Resources Board (CARB) inventories (thick lines; right axis labels) for fossil fuel-
 1070 derived emissions with top-down [annual](#) averages from the Pasadena data, using the
 1071 Miller and Tans (2003) approach to attribute CO₂ emissions from petroleum and natural
 1072 gas combustion from the $\delta^{13}\text{C}$ measurements. [Annual](#) curves showing the attribution of
 1073 C_x, [averaged from the seasonal values](#) from Fig. 6b are shown as thin [ner](#) lines. [The error](#)
 1074 [bars on the results from the flask sample data are 1 \$\sigma\$ standard errors of the means](#). The
 1075 annual trends from the bottom-up CARB inventories are plotted on a scale exactly 100
 1076 times that of the trends derived from the CO₂ measurements, showing that the relative
 1077 proportions are very similar through 2013.



1078 | Figure 12. Comparison of the Pasadena C_{pet} atmospheric concentration with all available
 1079 | area-integrated bottom-up fossil fuel CO_2 emissions per month (mo), including gasoline
 1080 | sales based on taxes paid to the California Board of Equalization (CBE, 2014), gasoline
 1081 | provided in California by prime suppliers, the California Air Resources Board's annual
 1082 | road emissions (CARB, 2015), and the Hestia-LA gridded total petroleum. The Hestia-
 1083 | LA data product is specific to the Los Angeles megacity domain; all inventories are
 1084 | statewide estimates. Since the Hestia-LA product is gridded, we show the emissions
 1085 | emanating from different regions for January (northeast quadrant, Fig. 13a) and July
 1086 | (southwest quadrant), based on prevailing winds during those periods (Figs. 7 and 13a).
 1087 | The axis for each inventory has been adjusted to allow easy comparison. The seasonality
 1088 | of the C_{pet} data lags the bottom-up inventories by a few months. This analysis is
 1089 | consistent with the observed decrease in gasoline combustion during 2008-2011.